RADBOUD UNIVERSITY NIJMEGEN

FACULTY OF SCIENCE (FNWI)

THEORETICAL HIGH ENERGY PHYSICS

Effectiveness of renormalisation in zero-dimensional quantum electrodynamics

Author:
Ilija MILUTIN

Supervisor:
Prof. dr. Ronald KLEISS

July 2019

Abstract

In this research, the behaviour of the numerical coefficients in the polynomial expansion in $\hbar$ of the connected Green's functions before and after renormalisation were compared. In particular, this was done for a zero-dimensional toy model for quantum electrodynamics consisting of three quantum fields. The connected Green's functions were extracted from the field functions determined by iteration of the Schwinger-Dyson equations. The ratio between the numerical coefficients of the connected Green's functions before and after renormalisation approach a constant value for large powers of $\hbar$. The coefficients are approximately a factor 33 smaller than before renormalisation, which is in agreement with theoretical predictions by Borinsky.[1] Furthermore, this process was repeated with the tadpole diagrams removed from the connected Green's functions. Similarly, the ratio approaches a constant value and the numerical coefficients are approximately a factor 12 smaller than before renormalisation. This is in accordance with the theoretical prediction by Borinsky for the inclusion of Furry's theorem[1], thus showing that in the asymptotic regime the effect of Furry's theorem is dominated by tadpole diagrams.

Contents

1 Introduction

In this research, a zero-dimensional toy model for quantum electrodynamics (QED) will be studied. This will serve as a primitive model for the theory of electrons, positrons and photons. In particular, the effects of renormalisation on the numerical coefficients in the polynomial expansion in $\hbar$ of the connected Green's functions will be analysed. These numerical coefficients behave as a divergent series before renormalisation.
The topic of this research was inspired by the research done by Dirk van Buul in [2], where renormalisation in φ^4 theory still yielded a divergent series of coefficients. However, the coefficients decreased by a factor of approximately 40 in the limit of large powers of $\hbar$ after renormalisation.[2] This was in agreement with the theoretical prediction of $e^{-15/4}$.[3]
I was interested if in a more complicated (toy) model, like QED, such a factor also can be found. Namely, in QED one has three quantum fields instead of one as in φ^4 theory. Furthermore, other properties like tadpole diagrams and Furry's theorem play a role in QED, unlike in φ^4 theory.
The approach for this research consists of using the Schwinger-Dyson equation (SDe) as a starting point for calculating all the necessary functions. By using the language of Feynman diagrams, a more intuitive approach is given to understand the SDe's, connected Green's functions and tadpole diagrams.
In Section 2, the theoretical concepts of quantum field theory and Feynman diagrams needed to understand this research are explained. The concepts and methods used in the renormalisation process used in this research are outlined in Section 3. After this, the results of this research will be presented and discussed.

2 Theory

2.1 Quantum field theory

Quantum field theory includes both special relativity and quantum mechanics to describe particles, in particular by using objects called quantum fields. The basic model that will be used for QED in this research is taken from [3] en consists of three quantum fields: φ, $\overline{\varphi}$ and B. In zero dimensions these three fields each assign a real number to a single point. These fields are stochastic variables, thus all that can be known are its combined probability density $P(\varphi,\overline{\varphi},B)$ and its moments $\langle\varphi^{n_1}\overline{\varphi}^{n_2}B^{n_3}\rangle$. The probability density is given by

$$P(\varphi,\overline{\varphi},B) = N\exp\left(-\frac{1}{\hbar}S(\varphi,\overline{\varphi},B)\right) \quad , \tag{1}$$

where N is a normalisation constant and the function $S(\varphi,\overline{\varphi},B)$ is called the action. This function $S(\varphi,\overline{\varphi},B)$ defines the theory. The variable $\hbar$ will be elaborated upon when discussing Feynman diagrams. For the primitive model of QED in this research the following action was used:

$$S(\varphi,\overline{\varphi},B) = \frac{1}{2}\mu B^2 + m\varphi\overline{\varphi} + e\overline{\varphi}B\varphi \quad , \tag{2}$$

where μ, m and e are the parameters of the model (which will be renormalised), the first two terms are the kinetic terms and the third term is an interaction term of the fields. Thus one can see e as a coupling constant. The moments of the quantum fields, also called Green's functions, are given by

$$G_{n_1,n_2,n_3} \equiv \langle\varphi^{n_1}\overline{\varphi}^{n_2}B^{n_3}\rangle \equiv N\iiint \exp\left(-\frac{1}{\hbar}S(\varphi,\overline{\varphi},B)\right)\varphi^{n_1}\overline{\varphi}^{n_2}B^{n_3}\,d\varphi d\overline{\varphi}dB \quad , \tag{3}$$

where N is a normalisation constant, the integrals are taken from $-\infty$ to $+\infty$ [i] and the n_i's are non negative integers. By definition we have $G_{0,0,0} = 1$. It is helpful to express these Green's functions in the form of a generating function. This generating function is called the path integral and is defined as

$$\begin{aligned} Z(\overline{J},J,H) &\equiv \sum_{n_1,n_2,n_3\geq 0}\frac{1}{n_1!}\left(\frac{\overline{J}}{\hbar}\right)^{n_1}\frac{1}{n_2!}\left(\frac{J}{\hbar}\right)^{n_2}\frac{1}{n_3!}\left(\frac{H}{\hbar}\right)^{n_3}G_{n_1,n_2,n_3} \\ &= N\iiint \exp\left(-\frac{1}{\hbar}\left(S(\varphi,\overline{\varphi},B)-\overline{J}\varphi-J\overline{\varphi}-HB\right)\right)d\varphi d\overline{\varphi}dB \quad , \end{aligned} \tag{4}$$

where the last three terms in the exponent include the sources of the fields, which will become clearer when we discuss Feynman diagrams. All the information of the three fields is contained in the Green's functions and thus also in the path integral. We can also define $W(\overline{J},J,H)$ as the logarithm of the path integral:

$$\begin{aligned} W(\overline{J},J,H) &\equiv \ln Z(\overline{J},J,H) \\ &= \sum_{n_1,n_2,n_3\geq 0}\frac{1}{n_1!}\left(\frac{\overline{J}}{\hbar}\right)^{n_1}\frac{1}{n_2!}\left(\frac{J}{\hbar}\right)^{n_2}\frac{1}{n_3!}\left(\frac{H}{\hbar}\right)^{n_3}C_{n_1,n_2,n_3} \quad , \end{aligned} \tag{5}$$

where C_{n_1,n_2,n_3} are the connected Green's functions. By definition we have $C_{0,0,0} = 0$. The connected Green's functions C_{n_1,n_2,n_3} are the cumulants of the probability density given by Equation 1. In this research, the effect of the renormalisation of the three parameters μ, m and e on the polynomial expansion in $\hbar$ of these connected Green's

[i] This convention will be used throughout this entire article.

functions is the main point of interest. Since $C_{0,0,0} = 0$, all the information about the probability density given in Equation 1 is also contained in the derivatives of $W(\bar{J}, J, H)$, which are called the field functions and are given by

$$\begin{aligned} \psi &= \hbar \frac{\partial}{\partial \bar{J}} W(\bar{J}, J, H) \quad , \\ \overline{\psi} &= \hbar \frac{\partial}{\partial J} W(\bar{J}, J, H) \quad , \\ A &= \hbar \frac{\partial}{\partial H} W(\bar{J}, J, H) \quad . \end{aligned} \tag{6}$$

The derivative of $W(\bar{J}, J, H)$ with respect to the source of the quantum field (in Equation 4 the sources are multiplied with their respective fields) gives the field function corresponding with that certain quantum field. The general form of these field functions is

$$\psi = \sum_{n_1, n_2, n_3 \geq 0} \frac{1}{n_1!} \left(\frac{\bar{J}}{\hbar} \right)^{n_1} \frac{1}{n_2!} \left(\frac{J}{\hbar} \right)^{n_2} \frac{1}{n_3!} \left(\frac{H}{\hbar} \right)^{n_3} C_{n_1+1, n_2, n_3} \quad , \tag{7}$$

where for $\overline{\psi}$ or A one replaces C_{n_1+1,n_2,n_3} with C_{n_1,n_2+1,n_3} or C_{n_1,n_2,n_3+1} respectively. In this form we can see that we can extract the connected Green's functions by looking at the corresponding powers of $\bar{J}$, J and H in the field functions.

2.2 Schwinger-Dyson equation

A useful way to describe the field functions is the Schwinger-Dyson equation (SDe). The derivation of the general form of the SDe can be found in [3], whereas here only the relevant results are discussed. The SDe for the path integral for an arbitrary number of quantum fields is given by

$$\left[\frac{\partial}{\partial \varphi_k} S(\varphi_1, \ldots, \varphi_K) \right]_{\varphi_j = \hbar \frac{\partial}{\partial J_j}} Z(J_1, \ldots, J_K) = J_k Z(J_1, \ldots, J_K) \quad . \tag{8}$$

Using Equation 8 in combination with Equations 2, 5 and 6 one finds the SDe's for the field functions:

$$\begin{aligned} \psi &= \frac{1}{m} J - \frac{e}{m} (\psi A + \hbar \frac{\partial}{\partial H} \psi) \quad , \\ \overline{\psi} &= \frac{1}{m} \bar{J} - \frac{e}{m} (\overline{\psi} A + \hbar \frac{\partial}{\partial H} \overline{\psi}) \quad , \\ A &= \frac{1}{\mu} H - \frac{e}{\mu} (\psi \overline{\psi} + \hbar \frac{\partial}{\partial J} \psi) \quad . \end{aligned} \tag{9}$$

We have used that the field functions are derivatives of $W(\bar{J}, J, H)$ and thus can write

$$\frac{\partial}{\partial J} A = \frac{\partial}{\partial H} \overline{\psi} \tag{10}$$

and other similar expressions for different combinations of the three field functions. In the next section, we will see that one can use Feynman diagrams for a more intuitive derivation of these SDe's. Solving the SDe's for the field functions given in Equation 9 is the basis of this research to obtain the field functions from which we can extract the connected Green's functions. The field functions can be found by iterating the SDe's in Equation 9 with $\psi = 0$, $\overline{\psi} = 0$ and $A = 0$ as a starting point. Each iteration adds a higher order term in perturbation theory.

2.3 Feynman diagrams

Another way to calculate the Green's functions, connected Green's functions and derive the SDe's for the field functions is by means of Feynman diagrams. A Feynman diagram is converted to a mathematical expression (which translates to the probability amplitude in four dimensions) by the use of Feynman rules. In the zero-dimensional model of QED used in this research the used Feynman rules are given in Figure 1. Important to note is that the

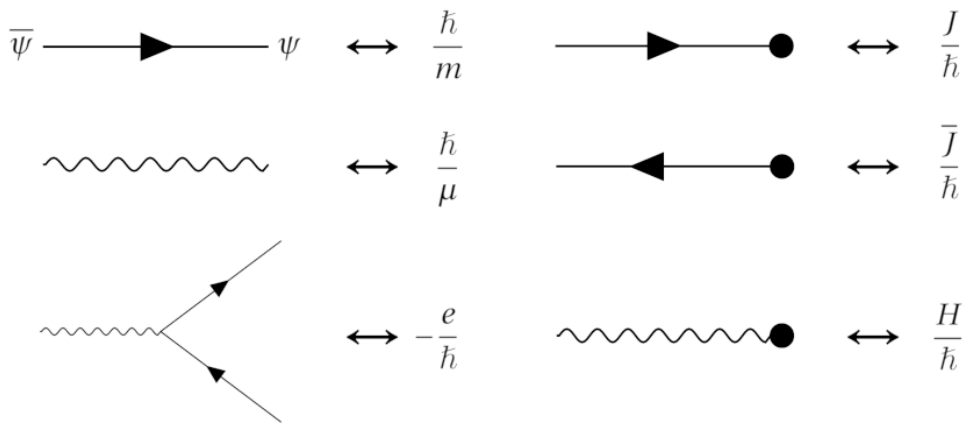

Figure 1: An overview of the Feynman rules for the QED model used. Note that the lines are not necessarily straight and that only the way lines and vertices are connected is relevant.

shape of the lines and the exact position of the vertices is irrelevant in our case. The diagrams do not represent 'moving particles', which is logical since there is no concept of movement in zero dimensions. In our case, only the way the lines and vertices are connected is relevant.
To find the mathematical expression of a Feynman diagram, all connected components are multiplied by each other and all graphs in a set are added together. Furthermore, one needs to take into account symmetry and multiplicity factors, for which an explanation can be found in [3]. The variable $\hbar$ represents the order of magnitude of the diagrams, which depends on the complexity of the diagrams. This is done by assigning a factor $\hbar$ to every closed loop. This $\hbar$ becomes the familiar reduced Planck's constant in four dimensions. This convention has already been incorporated in the Feynman rules given in Figure 1.
Moreover, the field functions correspond with the diagrams given in Figure 2. The shaded blobs in Figure 2 represent all connected diagrams with any number of source vertices and no external lines (lines not ending in vertices). The derivation for this correspondence can be found in [3].
One can 'expand' the diagrams for the field functions intuitively by drawing the possible diagrams one encounters when following the single external line attached to it. By doing this we obtain the relations shown in Figure 3. One can derive that adding an external line to the diagram of a field function corresponds with taking the derivative of the field function with respect to the source of the corresponding added external line.[3] Since there are no symmetry or multiplicity factors to be taken in account in the diagrammatic equations shown in Figure 3, one can easily verify that the equations in Figure 3 correspond exactly to the SDe's for the field functions given in Equation 9.
It is also possible to derive that the connected Green's functions C_{n_1,n_2,n_3} correspond to all Feynman diagrams with n_1, n_2 and n_3 external lines of ψ, $\overline{\psi}$ and A respectively.[3] When expanding the connected Green's functions C_{n_1,n_2,n_3} in $\hbar$, the numerical coefficients in the polynomial expansion correspond with the number of distinct Feynman diagrams one can draw of a specific order, with the number of external lines given by the n_i's.

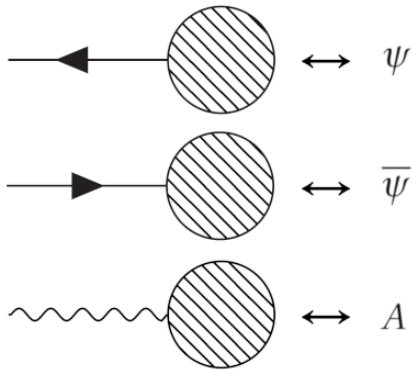

Figure 2: The Feynman diagrams representing the three field functions. The shaded blobs represent all connected diagrams with any number of sources and no external lines (except for the one attached to it). Note that the lines are not necessarily straight lines.

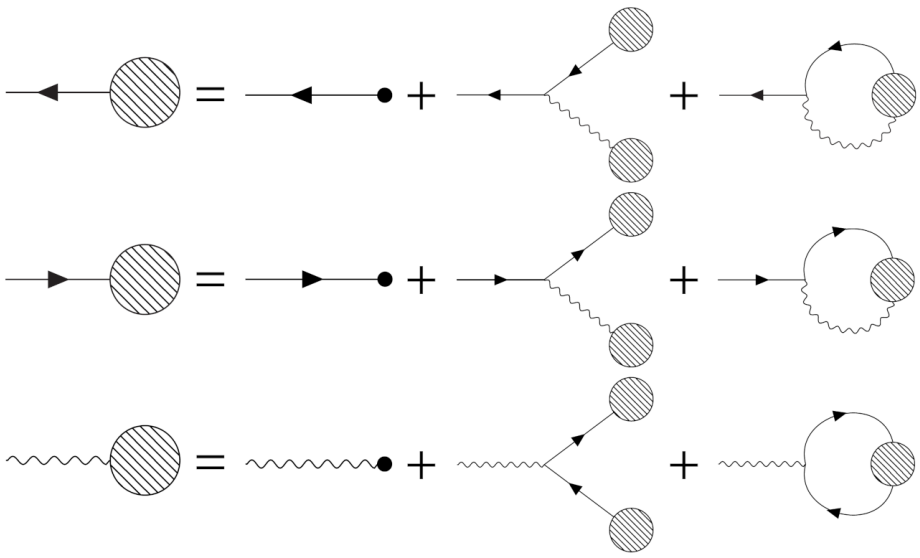

Figure 3: The SDe's for the three field functions represented by Feynman diagrams. Note that the lines are not necessarily straight lines.

3 Renormalisation

In this section the principles of renormalisation will be explained. I have presented it in such a way that it represents the methods used to find the desired results. The Maple code used to implement these methods can be found in Appendix A.

3.1 General methods

Renormalisation is the order-by-order updating of the parameters, which are μ, m and e in our model. It is necessary to renormalise these parameters since we apply perturbation theory to find our desired expressions for e.g. the connected Green's functions. The principles of renormalisation are best explained by giving an outline of how it was implemented in the simple QED model of this research.

3.1.1 Finding the field functions and connected Green's functions

As mentioned, one can iterate the SDe's for the field functions given in Equation 9. The method used for iteration is adapted from [2]. Firstly, ψ, $\overline{\psi}$ and A are set to 0 and Equation 9 is iterated. After a sufficient number of iterations, the field functions are found as a truncated polynomial expansion in $\hbar$.
Using Equation 7 one can now extract the connected Green's functions. In this research all C_{n_1,n_2,n_3} with $n_1+n_2+n_3 \leqslant 8$ have been determined. One would expect that all connected Green's functions with $n_1 \neq n_2$ will equal 0, because of fermion conservation. Looking at the connected Green's functions which have been found, one exactly sees that $C_{n_1,n_2,n_3} = 0$ if $n_1 \neq n_2$. In Equation 11 several connected Green's function are presented:

$$
\begin{aligned}
C_{0,0,1} &= -\frac{e\hbar}{\mu m} - 2\frac{e^3\hbar^2}{\mu^2 m^3} - 10\frac{e^5\hbar^3}{\mu^3 m^5} - 74\frac{e^7\hbar^4}{\mu^4 m^7} - 706\frac{e^9\hbar^5}{\mu^5 m^9} - 8162\frac{e^{11}\hbar^6}{\mu^6 m^{11}} - 110410\frac{e^{13}\hbar^7}{\mu^7 m^{13}} + \mathcal{O}(\hbar^8) \quad , \\
C_{0,0,2} &= \frac{\hbar}{\mu} + \frac{e^2\hbar^2}{\mu^2 m^2} + 6\frac{e^4\hbar^3}{\mu^3 m^4} + 50\frac{e^6\hbar^4}{\mu^4 m^6} + 518\frac{e^8\hbar^5}{\mu^5 m^8} + 6354\frac{e^{10}\hbar^6}{\mu^6 m^{10}} + 89782\frac{e^{12}\hbar^7}{\mu^7 m^{12}} + \mathcal{O}(\hbar^8) \quad , \\
C_{1,1,0} &= \frac{\hbar}{m} + 2\frac{e^2\hbar^2}{\mu m^3} + 10\frac{e^4\hbar^3}{\mu^2 m^5} + 74\frac{e^6\hbar^4}{\mu^3 m^7} + 706\frac{e^8\hbar^5}{\mu^4 m^9} + 8162\frac{e^{10}\hbar^6}{\mu^5 m^{11}} + 110410\frac{e^{12}\hbar^7}{\mu^6 m^{13}} + \mathcal{O}(\hbar^8) \quad , \\
C_{1,1,1} &= -\frac{e\hbar^2}{\mu m^2} - 6\frac{e^3\hbar^3}{\mu^2 m^4} - 50\frac{e^5\hbar^4}{\mu^3 m^6} - 518\frac{e^7\hbar^5}{\mu^4 m^8} - 6354\frac{e^9\hbar^6}{\mu^5 m^{10}} - 89782\frac{e^{11}\hbar^7}{\mu^6 m^{12}} + \mathcal{O}(\hbar^8) \quad . \qquad (11)
\end{aligned}
$$

The goal of this research is to compare the behaviour of the numerical coefficients in the polynomial expansion in $\hbar$ of the connected Green's functions before and after renormalisation.
Evaluating the integral in Equation 3 by treating $\overline{\varphi}$ as the complex conjugate of φ and using $G_{0,0,0} = 1$, gives

$$
G_{n,n,k} = \begin{cases} \dfrac{1}{N}\dfrac{\hbar^{n+\frac{k}{2}}}{\mu^{\frac{k}{2}} m^n} \displaystyle\sum_{l\geqslant 0} \frac{(2l+k)!\cdot(2l+n)!}{(2l)!\cdot(l+\frac{k}{2})!\cdot 2^{l+\frac{k}{2}}} \left(\frac{e^2\hbar}{\mu m^2}\right)^l & \text{for } k \text{ even} \\ -\dfrac{1}{N}\dfrac{e\hbar^{n+\frac{k+1}{2}}}{\mu^{\frac{k+1}{2}} m^{n+1}} \displaystyle\sum_{l\geqslant 0} \frac{(2l+k+1)!\cdot(2l+n+1)!}{(2l+1)!\cdot(l+\frac{k+1}{2})!\cdot 2^{l+\frac{k+1}{2}}} \left(\frac{e^2\hbar}{\mu m^2}\right)^l & \text{for } k \text{ odd} \end{cases}
$$

$$
\text{with} \qquad N = \sum_{j\geqslant 0} \frac{(2j)!}{j!\cdot 2^j}\left(\frac{e^2\hbar}{\mu m^2}\right)^j \quad . \qquad (12)
$$

Furthermore, $G_{n_1,n_2,n_3} = 0$ when $n_1 \neq n_2$ as expected, just as for the connected Green's functions. The connected Green's functions are related to the Green's functions through expressions like:

$$\begin{aligned} G_{0,0,1} &= C_{0,0,1} \quad , \\ G_{1,1,0} &= C_{1,0,0}C_{0,1,0} + C_{1,1,0} \quad , \\ G_{1,1,1} &= C_{1,0,0}C_{0,1,0}C_{0,0,1} + C_{1,1,0}C_{0,0,1} + C_{1,0,1}C_{0,1,0} + C_{0,1,1}C_{1,0,0} + C_{1,1,1} \quad . \end{aligned} \tag{13}$$

The connected Green's functions found by iterating the SDe's are in agreement with the relations given in Equation 13 and the evaluated integral for the Green's functions given in 12.

3.1.2 Renormalising the parameters

First, we assume that the values for $C_{0,0,2}$, $C_{1,1,0}$ and $C_{1,1,1}$ have been found experimentally and denote them by $E_{0,0,2}$, $E_{1,1,0}$ and $E_{1,1,1}$ respectively. We further assume that the measured values equal the first terms of the connected Green's functions giving

$$C_{0,0,2} = E_{0,0,2} \equiv \frac{\hbar}{\mu_R} \quad , \qquad C_{1,1,0} = E_{1,1,0} \equiv \frac{\hbar}{m_R} \qquad \text{and} \qquad C_{1,1,1} = E_{1,1,1} \equiv \frac{-e_R\hbar^2}{\mu_R m_R^2} \quad . \tag{14}$$

The next step is to find the parameters μ, m and e as a function of the renormalised parameters μ_R, m_R and e_R. This explains why we need three measurements, since we need three independent equations to solve for our three parameters. If everything is done correctly, $C_{0,0,2}$, $C_{1,1,0}$ and $C_{1,1,1}$ should then reduce to Equation 14 up to the order that the renormalised parameters have been found. The behaviour of the other renormalised Green's functions is what we are interested in.
To find the renormalised parameters, we first note from Equation 11 that we can write the connected Green's functions as:

$$C_{0,0,2} = \frac{\hbar}{\mu} \cdot f_{0,0,2}(x) \quad , \qquad C_{1,1,0} = \frac{\hbar}{m} \cdot f_{1,1,0}(x) \qquad \text{and} \qquad C_{1,1,1} = \frac{-e\hbar^2}{\mu m^2} \cdot f_{1,1,1}(x) \quad , \tag{15}$$

where $x = \dfrac{e^2\hbar}{\mu m^2}$ and the f's are polynomials in x. Furthermore, we define $x_R = \dfrac{e_R^2\hbar}{\mu_R m_R^2}$. We now want to write x as a function of x_R. Looking at Equations 14 and 15, we see that we have

$$\frac{C_{1,1,1}^2}{C_{0,0,2} \cdot C_{1,1,0}^2} = \frac{x \cdot f_{1,1,1}(x)^2}{f_{0,0,2}(x) \cdot f_{1,1,0}(x)^2} = x_R \quad . \tag{16}$$

Using Maple we can invert this relation to find x as a function of x_R (denoted by $x = x(x_R)$). Inserting this in Equation 15 and using the definition of x_R, we find

$$\begin{aligned} C_{0,0,2} &= \frac{\hbar}{\mu} \cdot F_{0,0,2}\left(\frac{e_R^2\hbar}{\mu_R m_R^2}\right) = \frac{\hbar}{\mu_R} \quad , \\ C_{1,1,0} &= \frac{\hbar}{m} \cdot F_{1,1,0}\left(\frac{e_R^2\hbar}{\mu_R m_R^2}\right) = \frac{\hbar}{m_R} \quad , \\ C_{1,1,1} &= \frac{-e\hbar^2}{\mu m^2} \cdot F_{1,1,1}\left(\frac{e_R^2\hbar}{\mu_R m_R^2}\right) = \frac{-e_R\hbar^2}{\mu_R m_R^2} \quad , \end{aligned} \tag{17}$$

where the F's are polynomials. Rewriting Equation 17 gives the original parameters as a function of the renormalised parameters:

$$\begin{aligned}
\mu &= \mu_R \cdot F_{0,0,2}\left(\frac{e_R^2\hbar}{\mu_R m_R^2}\right) \quad , \\
m &= m_R \cdot F_{1,1,0}\left(\frac{e_R^2\hbar}{\mu_R m_R^2}\right) \quad , \\
e &= e_R \cdot F_{0,0,2}\left(\frac{e_R^2\hbar}{\mu_R m_R^2}\right) \cdot F_{1,1,0}\left(\frac{e_R^2\hbar}{\mu_R m_R^2}\right)^2 \cdot F_{1,1,1}\left(\frac{e_R^2\hbar}{\mu_R m_R^2}\right)^{-1} \quad .
\end{aligned} \tag{18}$$

Now one can use the expressions in Equation 18 to substitute μ, m and e for their renormalised versions in all connected Green's functions.

3.2 Tadpole renormalisation

One aspect of QED that this model does not take into account are tadpoles. Tadpoles are diagrams which have an incoming photon and no outgoing particles (and no sources). The simplest tadpole is shown in Figure 4. The

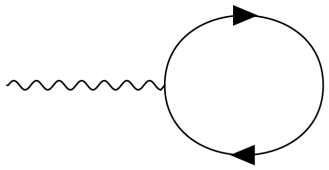

Figure 4: The Feynman diagram of the simplest tadpole. One can also have the same diagram with the fermion loop oriented in the opposite direction. Note that the lines are again not necessarily straight lines or perfect circles.

model that has been used assigns a value to each tadpole diagram according to the Feynman rules given in Figure 1. However, we know that the value of all these diagrams equal 0 (in our four dimensional world). There exists a very simple intuitive argument for why this holds. In four dimensions the probability amplitude of the Feynman diagrams are dependant on the four-momenta of the involved particles. Since at the end of a process represented by a tadpole diagram no particles are present, thus no four-momentum, one can conclude from four-momentum conservation that the initial four-momentum of the photon must equal 0. This is the reason why the value of all tadpole diagrams in our theory must equal 0. To correct this in our model, a counter term is subtracted from the SDe for the field function A in Equation 9. One then obtains the following SDe:

$$A = \frac{1}{\mu}H - \frac{e}{\mu}(\psi\overline{\psi} + \hbar\frac{\partial}{\partial J}\psi) - \frac{\hbar T}{\mu} \quad , \tag{19}$$

where the variable T is used to represent the tadpole diagrams. Visualising this with Feynman diagrams gives the SDe in Figure 5, where the crossed dot represents all connected Feynman diagrams with no sources and no external lines (except for the single photon attached to it). Another important thing to note is that the connected Green's function $C_{0,0,1}$ exactly describes all tadpoles. Namely, $C_{0,0,1}$ describes all connected diagrams with no sources with one photonic external line and no other external lines. Thus one needs to set $C_{0,0,1}$ equal to 0. To correct for the tadpoles in the other connected Green's functions (occurring as 'branches' in their Feynman diagrams), one first iterates the SDe's from Equation 9 with the additional counter term given in Equation 19 and extracts the

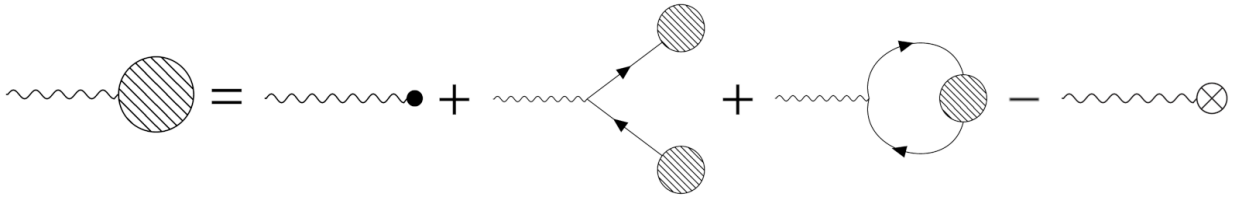

Figure 5: The SDe for the field function A with the counter term for the tadpole diagrams. The crossed dot represents all connected Feynman diagrams with no sources and no external lines. Note that the lines are again not necessarily straight lines.

connected Green's functions from the field functions. Then one solves $C_{0,0,1} = 0$ for T. We denote this solution as T_R. By performing the substitution $T = T_R$ in the other connected Green's functions one can remove the tadpole contributions from all connected Green's functions. For comparison, the same connected Green's functions (not renormalised) as in Equation 11, with the tadpole diagrams removed, are given by:

$$
\begin{aligned}
C_{0,0,1} &= \mathcal{O}(\hbar^{50}) \quad , \\
C_{0,0,2} &= \frac{\hbar}{\mu} + \frac{e^2\hbar^2}{\mu^2 m^2} + 4\frac{e^4\hbar^3}{\mu^3 m^4} + 27\frac{e^6\hbar^4}{\mu^4 m^6} + 248\frac{e^8\hbar^5}{\mu^5 m^8} + 2830\frac{e^{10}\hbar^6}{\mu^6 m^{10}} + 38232\frac{e^{12}\hbar^7}{\mu^7 m^{12}} + \mathcal{O}(\hbar^8) \quad , \\
C_{1,1,0} &= \frac{\hbar}{m} + \frac{e^2\hbar^2}{\mu m^3} + 4\frac{e^4\hbar^3}{\mu^2 m^5} + 27\frac{e^6\hbar^4}{\mu^3 m^7} + 248\frac{e^8\hbar^5}{\mu^4 m^9} + 2830\frac{e^{10}\hbar^6}{\mu^5 m^{11}} + 38232\frac{e^{12}\hbar^7}{\mu^6 m^{13}} + \mathcal{O}(\hbar^8) \quad , \\
C_{1,1,1} &= -\frac{e\hbar^2}{\mu m^2} - 4\frac{e^3\hbar^3}{\mu^2 m^4} - 27\frac{e^5\hbar^4}{\mu^3 m^6} - 248\frac{e^7\hbar^5}{\mu^4 m^8} - 2830\frac{e^9\hbar^6}{\mu^5 m^{10}} - 38232\frac{e^{11}\hbar^7}{\mu^6 m^{12}} + \mathcal{O}(\hbar^8) \quad . \qquad (20)
\end{aligned}
$$

As expected, the numerical coefficients in the connected Green's functions in Equation 20 are smaller than in Equation 11, since diagrams including tadpoles are removed.

4 Results

After renormalisation, we find the following expressions for the renormalised connected Green's functions used to find the renormalised parameters:

$$\begin{aligned} C_{0,0,2,R} &= \frac{1}{\mu_R}\hbar + \mathcal{O}(\hbar^{100}) \quad , \\ C_{1,1,0,R} &= \frac{1}{m_R}\hbar + \mathcal{O}(\hbar^{100}) \quad , \\ C_{1,1,1,R} &= -\frac{e_R}{\mu_R m_R^2}\hbar^2 + \mathcal{O}(\hbar^{100}) \quad . \end{aligned} \tag{21}$$

This is expected as this is the way the renormalisation procedure is defined.
Now that the connected Green's functions have been renormalised, the behaviour of the numerical coefficients in the polynomial expansion in $\hbar$ can be analysed. Since we are only interested in the numerical coefficients, we set all parameters (μ, m, e, μ_R, m_R and e_R) equal to 1, so that the connected Green's functions are given as polynomials in $\hbar$. We now introduce the following notation: $C^{(k)}_{n_1,n_2,n_3,R}$ is the absolute value of the coefficient of $\hbar^k$ in the polynomial expansion of $C_{n_1,n_2,n_3,R}$. In the exact same manner, we define $C^{(k)}_{n_1,n_2,n_3}$ for C_{n_1,n_2,n_3}. In this research the coefficients of all connected Green's functions C_{n_1,n_2,n_3} (and their renormalised versions) with $n_1+n_2+n_3 \leqslant 8$ have been determined. Due to fermion conservation, $C_{n_1,n_2,n_3} = C_{n_1,n_2,n_3,R} = 0$ if $n_1 \neq n_2$.

4.1 Tadpoles included

In this section, the results obtained without removing the tadpole diagrams will be presented. The SDe's have been iterated 100 times for the determination of the connected Green's functions in this section. In Figure 6a the logarithm of the coefficients $C^{(k)}_{0,0,8,R}$ and $C^{(k)}_{0,0,8}$ are plotted as a function of k. The behaviour of the other connected Green's functions is similar and thus not shown. It is clearly visible that the coefficients grow rapidly with k and that the coefficients of the renormalised connected Green's functions are smaller than those of the original connected Green's functions. Since the coefficients contain a factor of $k!$, the behaviour of the logarithm of $C^{(k)}_{0,0,8,R}$ and $C^{(k)}_{0,0,8}$ divided by $k!$ is shown in Figure 6b. By increasing the number of iterations of the SDe's, one can make plots like in Figure 6b and notice that the k corresponding with 'turning point' of the graph increases with the number of iterations used. This is expected since a higher number of iterations is needed to obtain the correct coefficients in higher order expansions of the connected Green's functions. In Figure 6b we can see that with 100 iterations, the coefficients up to approximately $k = 50$ have been accurately determined.

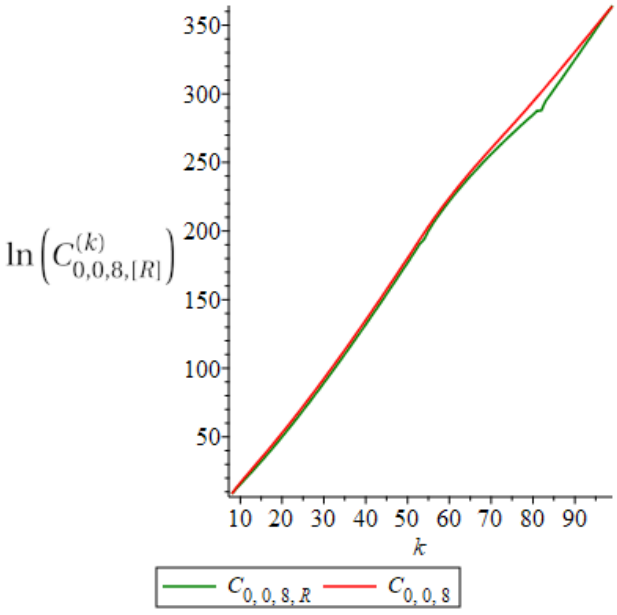

(a) The logarithm of the coefficients as a function of k.

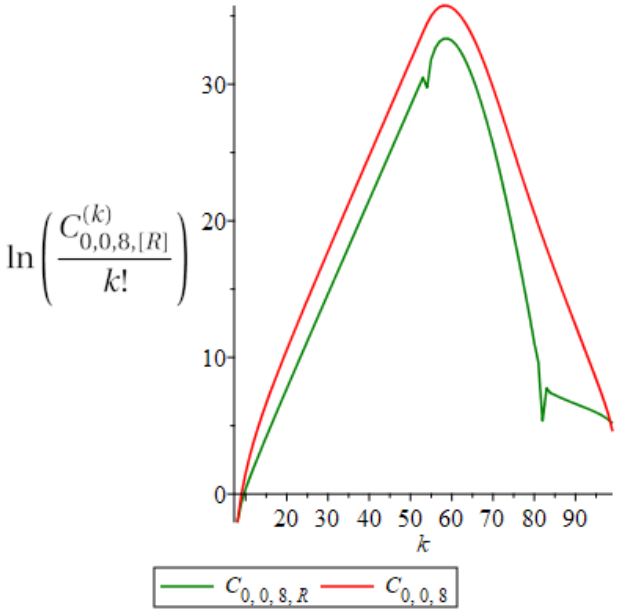

(b) The logarithm of the coefficients divided by $k!$ as a function of k.

Figure 6: The behaviour of the coefficients $C^{(k)}_{0,0,8,R}$ (green) and $C^{(k)}_{0,0,8}$ (red) as a function of the power k of $\hbar$ in the polynomial expansion of the connected Green's functions. The behaviour of the other connected Green's functions is similar and thus not shown.

To compare the behaviour of the coefficients in the renormalised connected Green's functions and the original connected Green's functions, the ratios between $C^{(k)}_{n_1,n_2,n_3,R}$ and $C^{(k)}_{n_1,n_2,n_3}$ have been plotted. Since the behaviour of the determined connected Green's functions are very similar, only the ratios of the connected Green's functions with $n_1 = n_2 = 0$ and $3 \leqslant n_3 \leqslant 8$ are shown in Figure 7. The plots for the other connected Green's functions can be found in Appendix B.

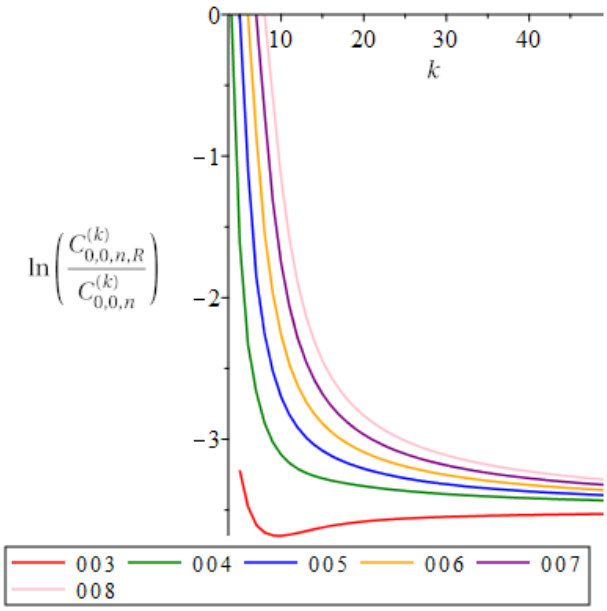

Figure 7: The logarithm of the ratios between $C^{(k)}_{0,0,n,R}$ and $C^{(k)}_{0,0,n}$ as a function of k. The legend shows the indices $n_1 n_2 n_3$ of the corresponding connected Green's functions.

In Figure 7 (and the figures in Appendix B), we can see that for large k

$$\ln\left(\frac{C^{(k)}_{n_1,n_2,n_3,R}}{C^{(k)}_{n_1,n_2,n_3}}\right) \approx constant \quad , \tag{22}$$

and that the ratios of the connected Green's functions with smaller indices approach this constant faster. This constant is approximately equal to $-\frac{7}{2}$, meaning that the coefficients for large k are approximately a factor 33 smaller after renormalisation. The numerical coefficients of the renormalised connected Green's functions are still a divergent series, but the ratio between the numerical coefficients of the renormalised connected Green's functions and the original connected Green's functions all seem to converge to a constant value.

4.2 Tadpoles excluded

In this section, the tadpole diagrams have been removed from the connected Green's functions. The SDe's have only been iterated 50 times, since due to the variable T introduced in the SDe's, the run time of the code used increases drastically as one increases the number of iterations and order up to which all variables are calculated. In this case, the equations in Equation 21 only hold up to order 50 instead of 100.
Similar to the last section, we can see in Figure 8 the behaviour of the coefficients $C^{(k)}_{0,0,8,R}$ and $C^{(k)}_{0,0,8}$. The other connected Green's functions again display similar behaviour and are thus not shown. From Figure 8b, we can conclude that, by using 50 iterations, the coefficients up to approximately $k = 25$ have been accurately determined. We can also see that the coefficients of the connected Green's functions are much smaller when the tadpole diagrams are removed. This is expected when one thinks of the connected Green's functions in Feynman diagrams: all diagrams where a photonic line ends in a closed diagram with no external lines are removed from to the connected Green's functions in Section 4.1.

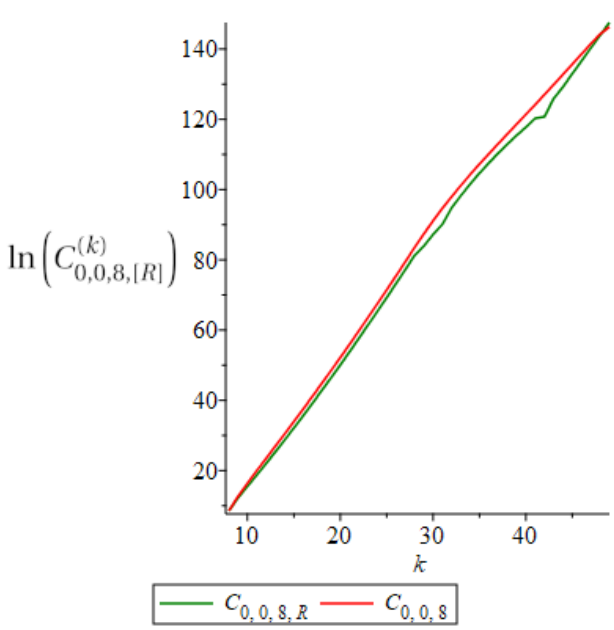

(a) The logarithm of the coefficients as a function of k.

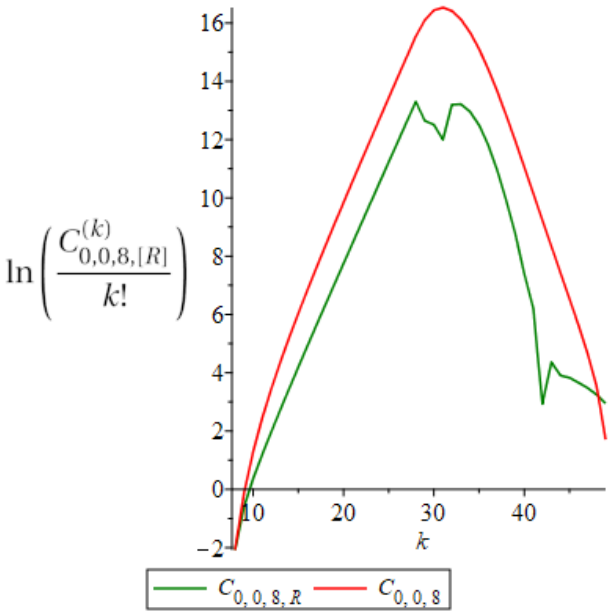

(b) The logarithm of the coefficients divided by $k!$ as a function of k.

Figure 8: The behaviour of the coefficients $C^{(k)}_{0,0,8,R}$ (green) and $C^{(k)}_{0,0,8}$ (red) as a function of the power k of $\hbar$ in the polynomial expansion of the connected Green's functions. Tadpole diagrams have been removed from these connected Green's functions. The behaviour of the other connected Green's functions is similar and thus not shown.

Similar to Section 4.1, the ratios between $C^{(k)}_{n_1,n_2,n_3,R}$ and $C^{(k)}_{n_1,n_2,n_3}$ have been determined. Since the behaviour of all determined connected Green's functions is similar, only the connected Green's functions with $n_1 = n_2 = 0$ and $3 \leqslant n_3 \leqslant 8$ are shown in Figure 9. The plots for the other connected Green's functions can be found in Appendix B. From these figures, we can again see that for large k

$$\ln\left(\frac{C^{(k)}_{n_1,n_2,n_3,R}}{C^{(k)}_{n_1,n_2,n_3}}\right) \approx constant \quad , \tag{23}$$

when removing the tadpole diagrams from the connected Green's functions. This constant is approximately equal to $-\frac{5}{2}$. Therefore, for large k the coefficients are approximately a factor 12 smaller after renormalisation. From these plots, we again see that the ratios of connected Green's functions with smaller indices approach this constant faster. As in the previous case, the numerical coefficients of the connected Green's functions still diverge, but their ratios converge to a larger constant when compared to the connected Green's functions including tadpole diagrams.

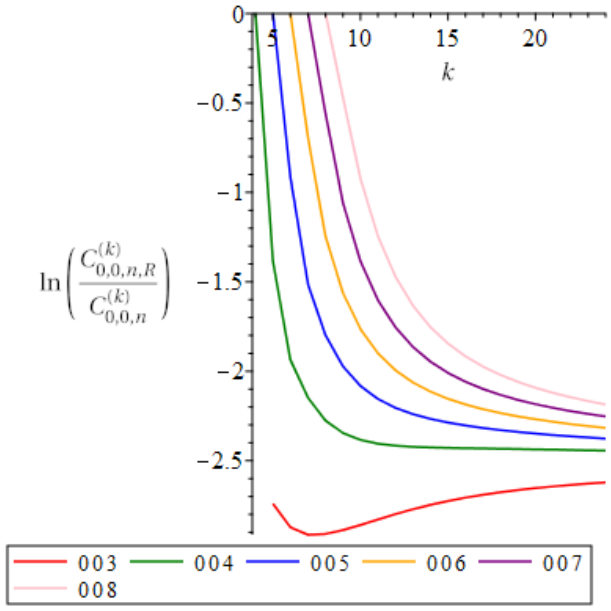

Figure 9: The logarithm of the ratios between $C^{(k)}_{0,0,n,R}$ and $C^{(k)}_{0,0,n}$ as a function of k. Tadpole diagrams have been removed from these connected Green's functions. The legend shows the indices $n_1\,n_2\,n_3$ of the corresponding connected Green's functions.

5 Discussion

From Figures 7 and 9, we see that the ratios between $C^{(k)}_{n_1,n_2,n_3,R}$ and $C^{(k)}_{n_1,n_2,n_3}$ approach a constant for large k. In the case where tadpole diagrams are not removed from the connected Green's functions, this constant is approximately $e^{-7/3}$. When these diagrams are removed, this constant is approximately $e^{-5/2}$. The numerical coefficients still behave as a divergent series, similar to the results found for φ^4 theory in [2].
As can be seen in Figures 7 and 9, all connected Green's functions seem to approach approximately the same constant value, but one needs to look at even higher order coefficients to provide more certainty for this statement. To improve the certainty of the values of the constants one needs to find the connected Green's functions up to an even higher order than in this research. This would also include increasing the number of iterations of the SDe's. Using the methods given in Appendix A, using another method of iterating the SDe's, or using another method instead of iterating the SDe's to find the connected Green's functions, one can try to increase the order up to which the coefficients have been found.
In [1], Borinsky derived mathematically from the path integral that the constant to which the ratios converge when including tadpole diagrams equals $e^{-7/2}$. This is confirmed by using the approach of iterating the SDe's used in this research. In Figure 7, one can see that the ratios all approach a value of approximately $e^{-7/2}$.
However, one aspect of QED has not been taken into account in both Sections 4.1 and 4.2. This is Furry's theorem.[1][4] Furry's theorem states that a Feynman diagram consisting of a fermion loop with n photonic lines attached to it, equals the same diagram with the fermion loop oriented the other way around times $(-1)^n$. This means that two identical diagrams with a fermion loop with an odd number of photonic lines attached to it and opposite orientations of the fermion loop, cancel each other out. By removing the tadpoles, only a subset of the diagrams in Furry's theorem have been removed from the connected Green's functions. To completely incorporate Furry's theorem in a similar manner by using counter terms in the SDe's, one would need to include a counter term for all uneven values of n which would result in infinitely many counter terms.
One can however make a substitution in the path integral to correct for Furry's theorem, of which the details are given in [1] and [4]. Here, only an intuitive argument will be given using Feynman diagrams and counter terms to clarify this substitution method. Firstly, we will write an expression for the Feynman diagrams consisting of one fermion loop with n photonic lines attached to it (but ignoring the propagator for B). Since there are n vertices and n fermion lines in each of these diagrams, every term includes a factor of $\left(-\frac{e}{m}\right)^n$. After fixing the first photonic line, there are $(n-1)!$ ways to attach the other photonic lines to the fermion loop, resulting in a factor of $(n-1)!$ in every term. To include counter terms for these loops, one needs to introduce n-point B self-interaction vertices, introducing a factor of $\frac{B^n}{n!}$ in every term.[3] All this information can be summed up in a logarithm:

$$\sum_{n\geqslant 1} \hbar(n-1)!\left(-\frac{e}{m}\right)^n \frac{B^n}{n!} = \sum_{n\geqslant 1} \hbar\left(-\frac{e}{m}\right)^n \frac{B^n}{n} = -\hbar\ln\left(1+\frac{eB}{m}\right) \quad , \tag{24}$$

where the $\hbar$ is added to include the loop-complexity. By performing the substitution in Equation 25, we find a counter term for the fermion loops with an odd number of photonic lines attached to it, thus incorporating Furry's theorem.

$$-\hbar\ln\left(1+\frac{eB}{m}\right) \to -\frac{\hbar}{2}\left(\ln\left(1+\frac{eB}{m}\right)-\ln\left(1-\frac{eB}{m}\right)\right) = \sum_{n\geqslant 0} \hbar\left(-\frac{e}{m}\right)^{2n+1} \frac{B^{2n+1}}{2n+1} \quad . \tag{25}$$

Borinsky calculated from the path integral using the substitution method, that the constant to which the ratio converges equals $e^{-5/2}$ when correcting for Furry's theorem. This corresponds with the ratio found when the tadpoles were removed, shown in Figure 9. Since the ratios of all the connected Green's functions seem to approach a value near $e^{-5/2}$ when removing the tadpole diagrams, we can conclude that in the asymptotic regime, the effects of

Furry's theorem are dominated by the tadpole diagrams.
This is expected since to mathematically derive the improvement factor, only the high order coefficients of the original connected Green's functions and the first lowest order renormalised terms of the connected Green's functions are required.[3] Since in the first few orders of perturbation theory (almost) all diagrams described by Furry's theorem are tadpole diagrams, the effects of Furry's theorem can be incorporated by only removing the tadpole diagrams.

6 Conclusion

Even after applying renormalisation, the numerical coefficients in the polynomial expansion in $\hbar$ of the connected Green's functions in our simple model of QED, still behave as a different series, but are smaller by a constant factor in the asymptotic regime of large powers of $\hbar$. When including tadpole diagrams in the connected Green's functions, this factor is approximately 33 and is close to the value calculated by Borinsky in [1]. When excluding the tadpole diagrams, one finds a factor of approximately 12. This is close to the value given by Borinsky in [1] when taking Furry' theorem into account in the model for QED. Tadpoles diagrams are a subset of the diagrams described in Furry's theorem. From this we can conclude that in the asymptotic regime, the effects of Furry's theorem are dominated by the tadpole diagrams.

References

[1] M. Borinsky, "Renormalized asymptotic enumeration of feynman diagrams", Annals of Physics **385**, 95–135 (2017).

[2] D. van Buul, "How effective is renormalization", bachelor thesis (2018).

[3] R. H. P. Kleiss, *Pictures, paths, particles, processes* (Radboud University, Nijmegen, Sept. 2018).

[4] P. Cvitanović, B. Lautrup, and R. B. Pearson, "Number and weights of feynman diagrams", Physical Review D **18**, 1939 (1978).

A Maple code

The code used for this project is given below. Since some variables used in the text are given another symbol in the code, Table 1 is included to show the correspondence between symbols in the text and in the code. Not all calculations of every connected Green's function are shown, since they are all based on Equation 7 (and the corresponding equations for $\overline{\psi}$ and A) and thus are all very similar. Furthermore, the part of the code concerning the plotting of the coefficients of the connected Green's functions are left out since these are trivial. Moreover, the variable u used in the code is a tool to group terms with the same sum of powers of the three sources. Finally, the code includes tadpole renormalization. To obtain the code used for renormalising the connected Green's function without tadpole renormalization, the term $u*h*T/\mu$ is removed from the SDe and all steps involving the variable T are ignored. Furthermore, the number 50 was changed to 100 when no tadpole renormalisation was implemented.

Table 1: Table showing the correspondence between symbols in the text and in the code. Only the symbols that differ are shown.

Symbol in the text	Symbol in the code
ψ	$psi1$
$\overline{\psi}$	$psi2$
$\overline{J}$	Y
$\hbar$	h
$x(x_R)$	S

```
restart;
psi1:=0:  psi2:=0:  A:=0:
for k from 1 to 50 do;
     psi1t:=u*J/m - e/m*(A*psi1 + h*diff(psi1,H));
     psi2t:=u*Y/m - e/m*(A*psi2 + h*diff(psi2,H));
     At:=u*H/mu - e/mu*(psi1*psi2 + h*diff(psi1,J)) - u*h*T/mu;
     psi1:=convert(expand(series(psi1t,u=0,k+1)),polynom);
     psi2:=convert(expand(series(psi2t,u=0,k+1)),polynom);
     A:=convert(expand(series(At,u=0,k+1)),polynom);
od:

A:=convert(subs(u=1,A),polynom):
psi1:=convert(subs(u=1,psi1),polynom):
psi2:=convert(subs(u=1,psi2),polynom):

for k from 0 to 8 do
     for l from 0 to 8 do
          for n from 0 to 8 do
               C[k,l,n]:=0;
          od:
     od:
od:

C[1,0,0]:=convert(series(subs(J=0,subs(Y=0,subs(H=0,psi1)))*h^(1+0+0-1),h=0,50),
polynom);
C[0,1,0]:=convert(series(subs(J=0,subs(Y=0,subs(H=0,psi2)))*h^(0+1+0-1),h=0,50),
polynom);
```

```
C[0,0,1]:=convert(series(convert(subs(J=0,convert(subs(Y=0,convert(subs(H=0,A),
polynom)),polynom)),polynom)*h^(0+0+1-1),h=0,50),polynom);
C[2,2,2]:=series(coeff(coeff(coeff(A,H,1),J,2),Y,2)*h^(2+2+2-1)*2*2,h=0,50);
C[3,3,2]:=series(coeff(coeff(coeff(psi1,Y,2),J,3),H,2)*h^(3+3+2-1)*3*2*2*2,
h=0,50);

T[R]:=series(solve(C[0,0,1]=0,T0,h=0,50):
C[1,1,1,T]:=series(subs(T=T[R],C[1,1,1]),h=0,50):
C[0,0,2,T]:=series(subs(T=T[R],C[0,0,2]),h=0,50):
C[1,1,0,T]:=series(subs(T=T[R],C[1,1,0]),h=0,50):

f[1,1,1]:=algsubs(e^2*h/(m^2*mu)=x,convert(series(C[1,1,1,T]/(-e*h^2/(mu*m^2)),
h=0,50),polynom)):
f[0,0,2]:=algsubs(e^2*h/(m^2*mu)=x,convert(series(C[0,0,2,T]/(h/mu),h=0,50),
polynom)):
f[1,1,0]:=algsubs(e^2*h/(m^2*mu)=x,convert(series(C[1,1,0,T]/(h/m),h=0,50),
polynom)):
K:=convert(series(x*f[1,1,1]^2/(f[0,0,2]*f[1,1,0]^2),x=0,50),polynom):
S:=convert(series(solve(series(K,x=0,50)=x[R],x),x[R]=0,50),polynom):
F[1,1,1]:=algsubs(x=S,f[1,1,1]):
F[0,0,2]:=algsubs(x=S,f[0,0,2]):
F[1,1,0]:=algsubs(x=S,f[1,1,0]):
F[1,1,1]:=convert(series(algsubs(x[R]=e[R]^2*h/(m[R]^2*mu[R]),F[1,1,1]),h=0,50),
polynom):
F[0,0,2]:=convert(series(algsubs(x[R]=e[R]^2*h/(m[R]^2*mu[R]),F[0,0,2]),h=0,50),
polynom):
F[1,1,0]:=convert(series(algsubs(x[R]=e[R]^2*h/(m[R]^2*mu[R]),F[1,1,0]),h=0,50),
polynom):

M:=series(convert(series(m[R]*F[1,1,0],h=0,50),polynom),h=0,50):
MU:=convert(series(mu[R]*F[0,0,2],h=0,50),polynom):
E:=convert(series(e[R]*F[1,1,0]^2*F[0,0,2]/F[1,1,1],h=0,50),polynom):
Minv:=convert(series(1/M,h=0,50),polynom):
MUinv:=convert(series(1/MU,h=0,50),polynom):

for k from 0 to 8 do
     for l from 0 to 8 do
          for n from 0 to 8 do
               C[k,l,n,P]:=convert(C[k,l,n,],polynom);
          od:
     od:
od:
```

```
for k from 0 to 8 do
     for l from 0 to 8 do
          for n from 0 to 8 do
               C[k,l,n,T]:=convert(series(subs(T=T[R],C[k,l,n,P]),h=0,50),
                polynom);
          od:
     od:
od:

for k from 0 to 8 do
     for l from 0 to 8 do
          for n from 0 to 8 do
               C[k,l,n,R]:=convert(series(subs(minv=Minv, muinv=MUinv, etemp=E,
                subs(mu=1/muinv,m=1/minv,e=etemp,C[k,l,n,T])),h=0,50),polynom);
          od:
     od:
od:
```

B Plots of other connected Green's functions

The plots of the ratios between the numerical coefficients $C^{(k)}_{n_1,n_2,n_3,R}$ and $C^{(k)}_{n_1,n_2,n_3}$ not shown in the main text are given here. In Figure 10, the ratios of the connected Green's functions including tadpole diagrams are shown. In Figure 11, the ratios of the connected Green's functions excluding tadpole diagrams are shown.

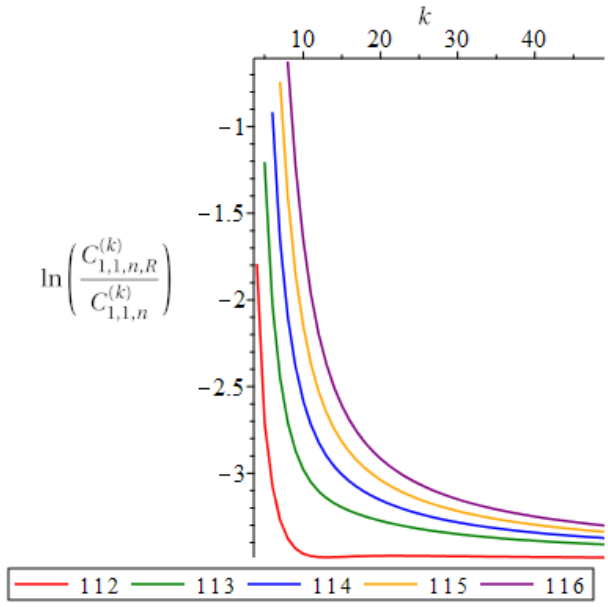

(a) The ratios of the connected Green's functions with $n_1 = n_2 = 1$ and $2 \leqslant n_3 \leqslant 6$.

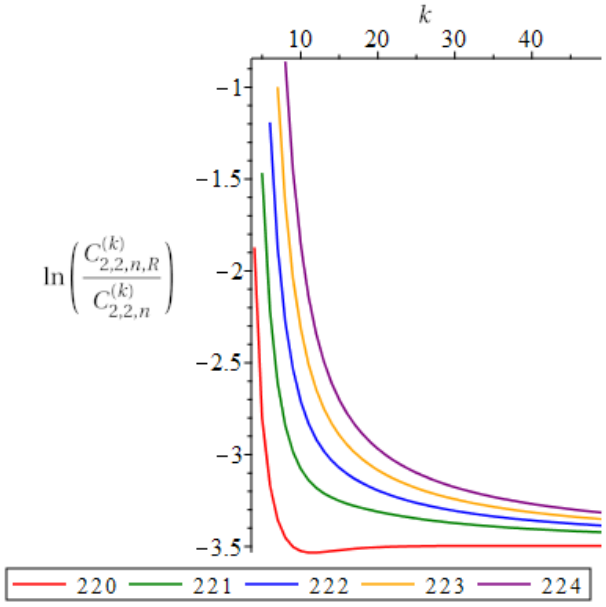

(b) The ratios of the connected Green's functions with $n_1 = n_2 = 2$ and $0 \leqslant n_3 \leqslant 4$.

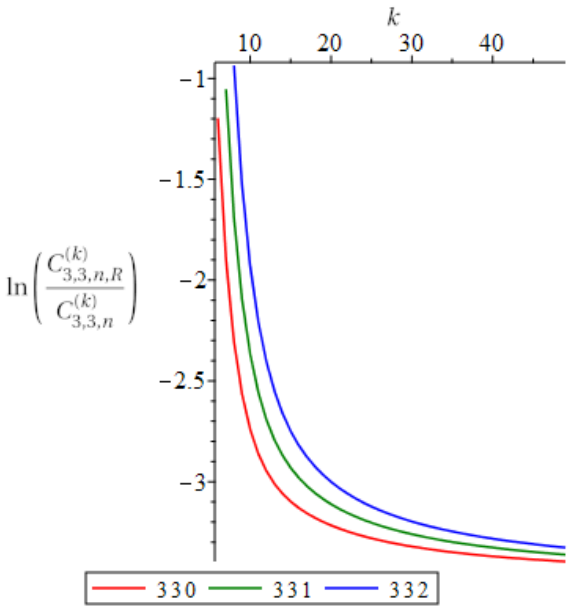

(c) The ratios of the connected Green's functions with $n_1 = n_2 = 3$ and $0 \leqslant n_3 \leqslant 2$.

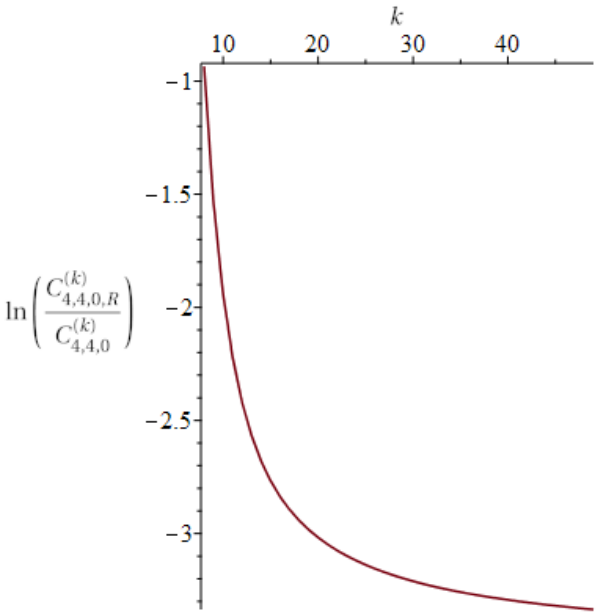

(d) The ratios of the connected Green's function with $n_1 = n_2 = 4$ and $n_3 = 0$.

Figure 10: The logarithm of the ratio between $C^{(k)}_{n_1,n_2,n_3,R}$ and $C^{(k)}_{n_1,n_2,n_3}$ as a function of k. Tadpole diagrams are included in the connected Green's functions in these plots. The legend shows the indices $n_1 n_2 n_3$ of the corresponding connected Green's functions.

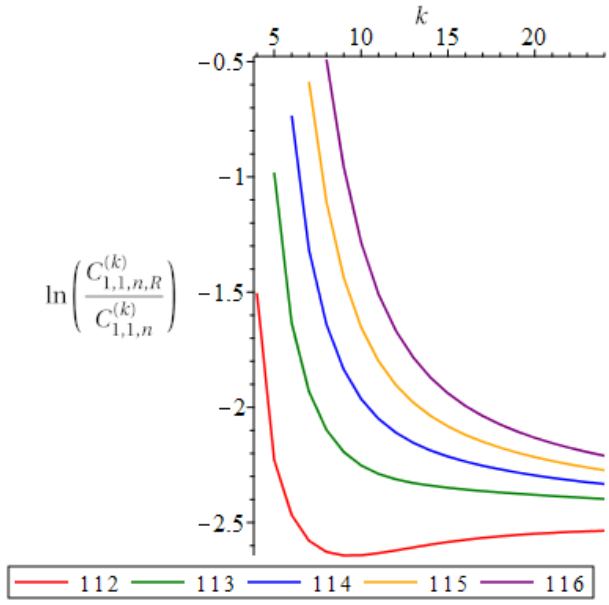

(a) The ratios of the connected Green's functions with $n_1 = n_2 = 1$ and $2 \leqslant n_3 \leqslant 6$.

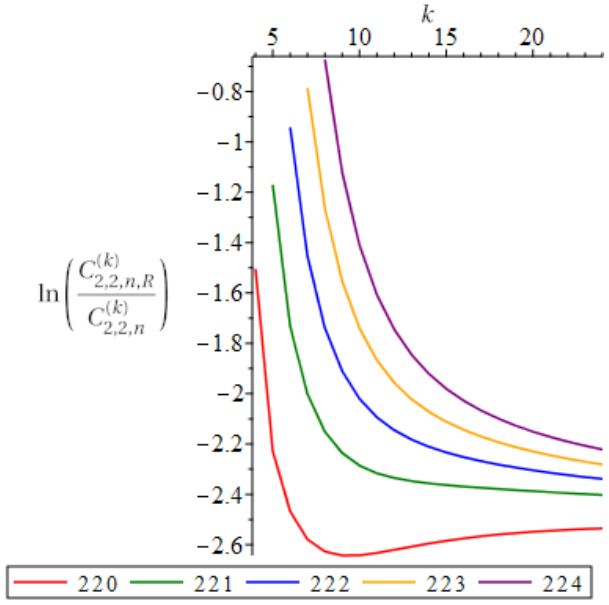

(b) The ratios of the connected Green's functions with $n_1 = n_2 = 2$ and $0 \leqslant n_3 \leqslant 4$.

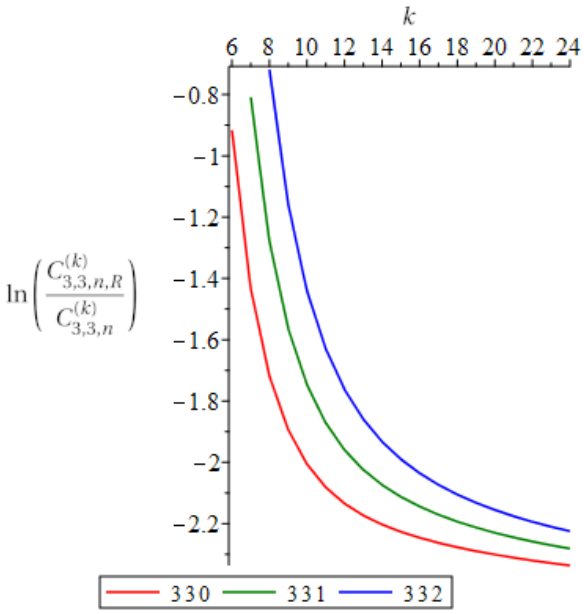

(c) The ratios of the connected Green's functions with $n_1 = n_2 = 3$ and $0 \leqslant n_3 \leqslant 2$.

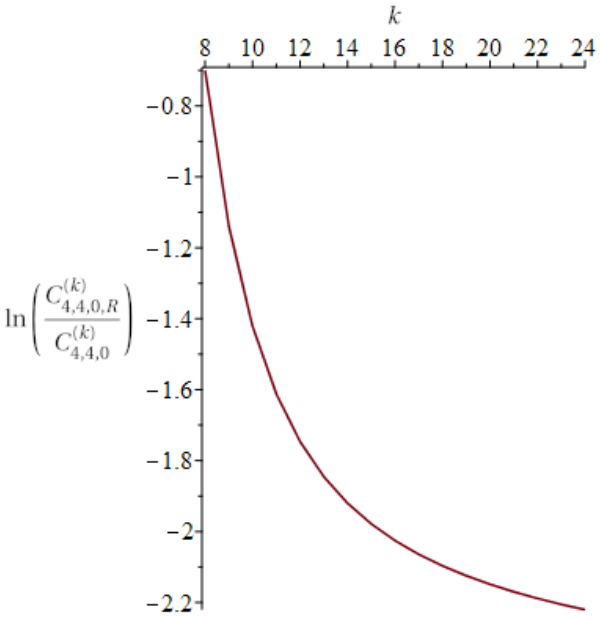

(d) The ratios of the connected Green's function with $n_1 = n_2 = 4$ and $n_3 = 0$.

Figure 11: The logarithm of the ratio between $C^{(k)}_{n_1,n_2,n_3,R}$ and $C^{(k)}_{n_1,n_2,n_3}$ as a function of k. Tadpole diagrams have been excluded from the connected Green's functions in these plots. The legend shows the indices $n_1 n_2 n_3$ of the corresponding connected Green's functions.